

Crossover to potential energy landscape dominated dynamics in a model glass-forming liquid

Thomas B. Schröder

Center for Theoretical and Computational Materials Science, National Institute of Standards and Technology, Gaithersburg, Maryland, 20899 and Department of Mathematics and Physics (IMFUFA), Roskilde University, P.O. Box 260, DK-4000 Roskilde, Denmark

Srikanth Sastry

Center for Theoretical and Computational Materials Science, National Institute of Standards and Technology, Gaithersburg, Maryland 20899 and Jawaharlal Nehru Centre for Advanced Scientific Research Jakkur Campus, Bangalore 560064, India

Jeppé C. Dyre

Department of Mathematics and Physics (IMFUFA), Roskilde University, P.O. Box 260, DK-4000 Roskilde, Denmark

Sharon C. Glotzer

Center for Theoretical and Computational Materials Science and Polymers Division, National Institute of Standards and Technology, Gaithersburg, Maryland 20899

(Received 8 November 1999; accepted 13 March 2000)

An equilibrated model glass-forming liquid is studied by mapping successive configurations produced by molecular dynamics simulation onto a time series of inherent structures (local minima in the potential energy). Using this “inherent dynamics” approach we find direct numerical evidence for the long held view that below a crossover temperature, T_x , the liquid’s dynamics can be separated into (i) vibrations around inherent structures and (ii) transitions between inherent structures [M. Goldstein, *J. Chem. Phys.* **51**, 3728 (1969)], i.e., the dynamics become “dominated” by the potential energy landscape. In agreement with previous proposals, we find that T_x is within the vicinity of the mode-coupling critical temperature T_c . We further find that near T_x , transitions between inherent structures occur via cooperative, stringlike rearrangements of groups of particles moving distances substantially smaller than the average interparticle distance. © 2000 American Institute of Physics. [S0021-9606(00)50122-6]

I. INTRODUCTION

Dynamical behavior of many physical and biological systems¹⁻⁴ can be considered in terms of the transient localization of the system in basins of potential energy, and transitions between basins. In particular, this approach has received much attention in studies of slow dynamics and the glass transition in supercooled liquids. Here, the strong temperature dependence of transport properties such as the diffusion coefficient and viscosity, and the possible existence of a thermodynamic transition underlying the laboratory glass transition, have been sought to be understood in terms of the properties of the liquid’s potential energy (or free energy) surface, or “landscape” as it is commonly called.^{1,2,5-18}

For a system composed of N atoms, the potential energy surface is simply the system’s potential energy plotted as a function of the $3N$ particle coordinates in a $3N+1$ dimensional space.⁵ The potential energy surface contains a large number of local minima, termed “inherent structures” by Stillinger and Weber.⁶ Each inherent structure is surrounded by a “basin,” which is defined such that a local minimization of the potential energy maps any point in the basin to the inherent structure contained within it. The time evolution of a liquid may be viewed as the motion of a point on the

potential energy surface, and thus as a succession of transitions from one basin to another. These transitions are expected to occur differently as the temperature T is varied. In particular, Goldstein argued⁵ that below a crossover temperature, T_x , where the shear relaxation time is $\sim 10^{-9}$ s, relaxation is governed by thermally activated crossings of potential energy barriers. The presence of significant energy barriers below T_x suggests a clear separation of short-time (vibrational) relaxation within potential energy basins from long-time relaxation due to transitions between basins.

A complementary approach to the dynamics of supercooled liquids is provided by the mode coupling theory (MCT).¹⁹ The simplest (so-called “ideal”) version of this theory predicts a power-law divergence of relaxation times and the inverse diffusion coefficient, at a critical temperature T_c . Although a power law provides a reasonable description of the temperature dependence of these quantities above T_c in both real and simulated systems, power law behavior breaks down for $T \approx T_c$, i.e., the predicted singularity at T_c is not observed. This deviation is attributed to the presence of “hopping” motion as a mechanism of relaxation, which is not included in ideal MCT.¹⁹ Consequently, T_c is usually estimated by fitting a power law to a relaxation time, taking

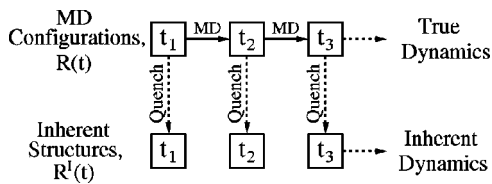


FIG. 1. Schematic describing the principle of the “inherent dynamics” approach. Successive configurations of the equilibrated liquid $\mathbf{R}(t)$ are quenched to produce their corresponding inherent structures $\mathbf{R}^I(t)$. Successive inherent structures form a time series which we use to calculate the inherent self intermediate scattering function $F_s^I(q,t)$ [Eq. (2.2)]. More generally, the inherent counterpart of any equilibrium quantity may be calculated in this fashion.

into account that this fit is expected to break down close to (and below) T_c .

It was noted by Angell⁷ that experimentally it is often found that the shear relaxation time is on the order of 10^{-9} s at the estimated T_c , leading to the argument that $T_x \approx T_c$ (See also Ref. 20). The presence of a low temperature regime where barrier crossings dominate the dynamics, and the correspondence of the crossover to that regime with the mode coupling critical temperature T_c , has also been discussed in the context of mean field theories of certain spin glass models.^{21–23}

The existence of the crossover temperature T_x and the corresponding separation of the dynamics can be directly tested with computer simulations, using the concept of inherent structures. In this paper, we map the dynamical evolution of an equilibrated model liquid to a time series of inherent structures for a range of temperatures. In this way, we test the extent to which short-time “intrabasin” relaxation is separable from long-time “interbasin” relaxation. Our results demonstrate that this separation becomes valid as the system is cooled, and we estimate the crossover temperature T_x to be close to the estimated value of T_c .

II. INHERENT DYNAMICS

In this section we describe the details of our approach, which is sketched in Fig. 1. After equilibration at a given thermodynamic state point, a discrete time series of configurations, $\mathbf{R}(t)$, is produced by standard molecular dynamics (MD) simulation. Each of the configurations $\mathbf{R}(t)$ is then mapped to its corresponding inherent structure, $\mathbf{R}^I(t)$, by locally minimizing the potential energy in configuration space. We refer to this procedure as a “quench.” After quenching the configurations in $\mathbf{R}(t)$, we have two “parallel” time series of configurations, $\mathbf{R}(t)$ and $\mathbf{R}^I(t)$. The time series $\mathbf{R}(t)$ defines the “true dynamics,” which is simply the usual (Newtonian) MD dynamics. In an analogous way, the time series $\mathbf{R}^I(t)$ defines the “inherent dynamics.” If a function quantifying some aspect of the true dynamics is denoted by $f(\mathbf{R}(t))$, then the corresponding function, $f(\mathbf{R}^I(t))$, of the inherent dynamics is calculated in exactly the same way, except using the time series of inherent structures. For example, the self-intermediate scattering function, $F_s(q,t)$, and the *inherent* self intermediate scattering function, $F_s^I(q,t)$, are defined by

$$F_s(q,t) \equiv \langle \cos \mathbf{q} \cdot (\mathbf{r}_j(t) - \mathbf{r}_j(0)) \rangle, \quad (2.1)$$

and

$$F_s^I(q,t) \equiv \langle \cos \mathbf{q} \cdot (\mathbf{r}_j^I(t) - \mathbf{r}_j^I(0)) \rangle, \quad (2.2)$$

where $\mathbf{r}_j^I(t)$ is the position of the j th particle in the inherent structure $\mathbf{R}^I(t)$ and $\langle \dots \rangle$ denotes an average over j and the time origin.

In this paper, we quantitatively compare $F_s(q,t)$ and $F_s^I(q,t)$ to test whether the dynamics of a binary Lennard-Jones mixture can be separated into vibrations around, and transitions between, inherent structures. If so, then $F_s^I(q,t)$ describes the relaxation of the liquid as described by $F_s(q,t)$, but with the effect of the vibrations removed. We show that this scenario becomes true below a crossover temperature, T_x , which is close to the lowest temperature simulated in the present work.

III. RESULTS

In the following we present results from molecular dynamics simulations of a binary Lennard-Jones mixture in three dimensions, equilibrated at eight different temperatures. The model used for the present simulations is described in Ref. 24. The system contains 251 particles of type A and 249 particles of type B interacting via a binary Lennard-Jones potential with parameters $\sigma_{BB}/\sigma_{AA}=5/6$, $\sigma_{AB}=(\sigma_{AA}+\sigma_{BB})/2$, and $\epsilon_{AA}=\epsilon_{AB}=\epsilon_{BB}$. The masses are given by $m_B/m_A=1/2$. The length of the sample is $L=7.28\sigma_{AA}$ and the potential was cut and shifted at $2.5\sigma_{\alpha\beta}$. All quantities are reported in reduced units; T in units of ϵ_{AA} , lengths in units of σ_{AA} and time in units of $\tau \equiv (m_B\sigma_{AA}^2/48\epsilon)^{1/2}$ (this was misprinted in Ref. 24). Adopting “argon units” leads to $\sigma_{AA}=3.4 \text{ \AA}$, $\epsilon/k_B=120 \text{ K}$, and $\tau=3 \times 10^{-13} \text{ s}$. The simulations were performed in the NVE ensemble using the leapfrog algorithm with a time step of 0.01τ , at constant reduced density, $\rho=1.296$. The quenching was performed using the conjugate gradient method.²⁵

We first briefly describe aspects of the true dynamics that demonstrate a qualitative change occurring in the temperature range investigated.

In Fig. 2 we show the quantity $4\pi r^2 G_{sA}(r,t_1)$, which is the distribution of displacements²⁶ of particles of type A during the time interval t_1 . We define t_1 as the time where the mean square displacement is unity, $\langle r^2(t_1) \rangle_A = 1$. At all temperatures the dynamics become diffusive ($\langle r^2(t) \rangle_A \propto t$) for $t \geq t_1$ (see inset), i.e., t_1 marks the onset of diffusivity. At the highest temperatures, $4\pi r^2 G_{sA}(r,t_1)$ agrees well with the Gaussian approximation [thick curve, $G_{sA}(r,t_1) \propto \exp(-3r^2/2)$]. As T is lowered, the distribution of particle displacements deviates from the Gaussian approximation, and a shoulder develops at the average interparticle distance ($r \approx 1.0$ in the adopted units), which at $T=0.59$ becomes a well-defined second peak. The second peak, observed also in other model liquids at low temperatures, indicates^{27,28} single particle “hopping” [see Fig. 3(a)]; particles stay relatively localized for a period of time (first peak), and then move approximately one interparticle distance, where they again become localized (second peak). Thus we see from Fig. 2 that as we approach our lowest simulated temperature T

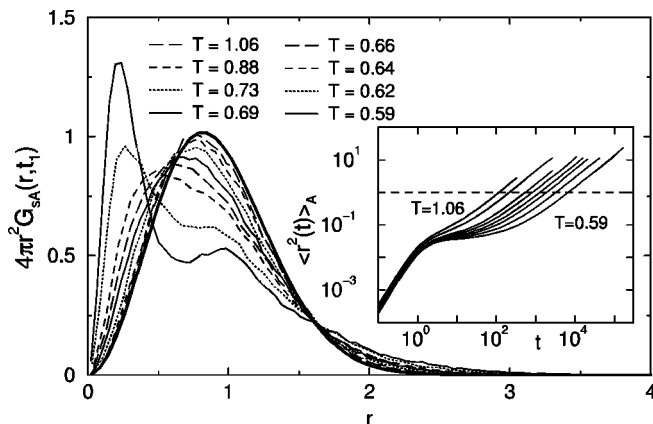


FIG. 2. Distribution of particle displacements for the A (large) particles, $4\pi r^2 G_{sA}(r, t_1)$, where t_1 is defined by $\langle r^2(t_1) \rangle_A = 1$ (see inset). At high T the Gaussian approximation (thick curve) is reasonable, whereas at the lowest T a second peak is present, indicating single particle hopping. (Inset) Mean square displacement of the A particles, $\langle r^2(t) \rangle_A$. Similar behavior is found for the B (small) particles.

$=0.59$, there is a qualitative change from dynamics well described by a Gaussian distribution to dynamics dominated by hopping processes.

In Fig. 3(b) the inherent dynamics approach is applied to the true trajectory seen in Fig. 3(a). The resulting “inherent trajectory” consists of the positions of the particle in 1600 successive quenched configurations. The quenching procedure is seen to remove the vibrational motion from the true trajectory. The inherent trajectory will be discussed in more detail in Sec. IV.

We now compare the true self intermediate scattering function, $F_s(q, t)$, with its inherent counterpart $F_s^I(q, t)$. Figure 4(a) shows the self-intermediate scattering function for the A particles, $F_{sA}(q, t)$, at $q=7.5$ corresponding to the position of the primary peak in the static structure factor for

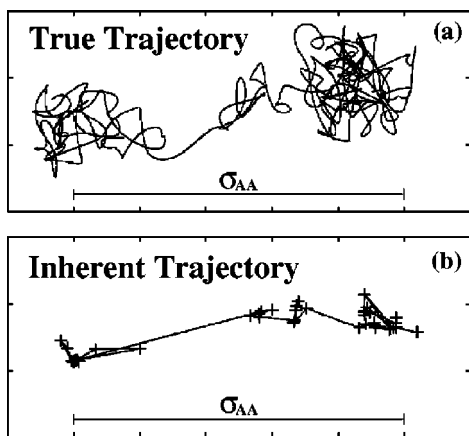


FIG. 3. (a) Trajectory of a particle at $T=0.59$. The elapsed time is $\Delta t = 160\tau$ (the typical “vibration” time is $\approx 1\tau$). At this temperature the dynamics is dominated by “hopping;” particles stay relatively localized for many time steps and then move approximately one interparticle distance, where they again become localized. (b) Applying the inherent dynamics approach to the trajectory above. The 1600 configurations used to generate the (true) trajectory in (a) were quenched, and the positions of the particle in the resulting inherent structures are here plotted and connected by straight lines.

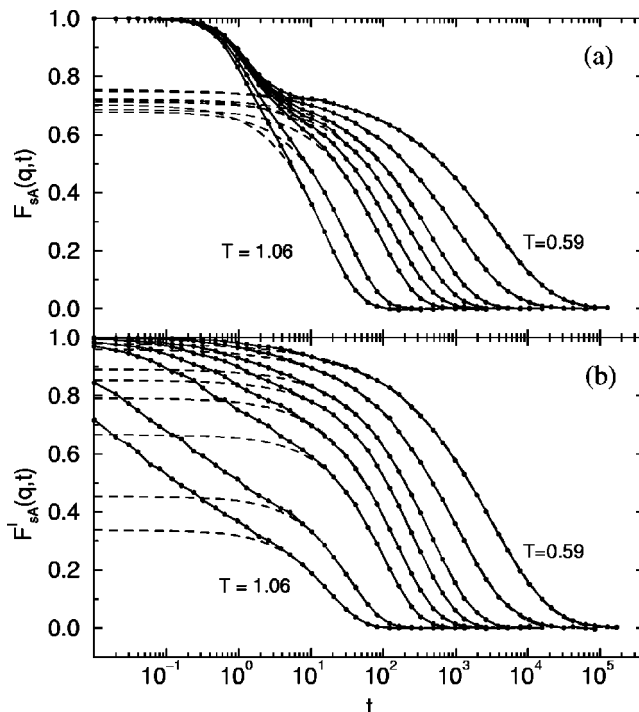


FIG. 4. (a) $F_{sA}(q, t)$ plotted vs t on the log-scale for $q=7.5$ at the same temperatures as in Fig. 2. Data points are connected by straight lines. Dashed lines are fits to $f(t) = f_c \exp(-t/\tau_c)^\beta$. (b) $F_{sA}^I(q, t)$, otherwise as above. In both (a) and (b), the fitting was performed for $t > 10$ for the two highest temperatures and for $t > 30$ otherwise. Similar behavior is found for the B particles.

the A–A correlation. For each temperature $F_s(q, t)$ was calculated from approximately 2000 configurations (depending on temperature). As T decreases, $F_{sA}(q, t)$ is found to display the typical two-step relaxation, where the short time decay is attributed to vibrational relaxation (or “dephasing,” see Ref. 11) of particles within cages formed by neighboring particles.^{29–31} The long time, or α -relaxation is separated from the short time regime by a plateau indicating transient localization, or “caging” of particles, and is generally observed to follow a stretched exponential form.

The self-part of the inherent intermediate scattering function for the A particles, $F_{sA}^I(q, t)$ at $q=7.5$, is shown in Fig. 4(b). This was calculated by quenching each configuration used in Fig. 4(a), and then applying the same data analysis program on the resulting time series of inherent structures. As expected, the plateau disappears in the inherent dynamics, as previously shown also for the inherent mean-square displacement.²⁴ At all T we find that the long-time behavior of both $F_{sA}(q, t)$ and $F_{sA}^I(q, t)$ is well described by stretched exponentials (dashed lines). As a result, we can quantitatively compare the long time relaxation of $F_{sA}(q, t)$ and $F_{sA}^I(q, t)$ by comparing the fitting parameters $\{\tau_\alpha, \beta, f_c\}$ of the stretched exponentials $f(t) = f_c \exp(-t/\tau_\alpha)^\beta$.

If the true dynamics can be separated into vibrations around and transitions between inherent structures, how do we expect the fitting parameters for the inherent self-intermediate scattering function, $\{\tau_\alpha^I, \beta^I, f_c^I\}$ to be related to the fitting parameters for the true self intermediate scattering function, $\{\tau_\alpha, \beta, f_c\}$? To answer this question, we assume

that the initial relaxation in $F_s(q,t)$ is due to vibrations (as widely accepted^{11,29-31}). If this is the case, then we expect the quenching procedure to remove the initial relaxation (since it removes the vibrations), which means that $F_s^l(q,t)$ can be thought of as $F_s(q,t)$ with the initial relaxation removed. If vibration can be separated from transitions between inherent structures we may write for the x -displacement, $\Delta x = \Delta x_{\text{vib}} + \Delta x_{\text{inh}}$, where the two terms are statistically uncorrelated. Thus, [using an exponential instead of cosine in Eqs. (2.1) and (2.2)] we find that the self-intermediate scattering function is a *product* of a term relating to vibrations and one relating to transitions between inherent structures. At long times the former becomes time-independent, converging to the nonergodicity parameter. This in turn means that $F_s^l(q,t)$ should be identical to the long time relaxation of $F_s(q,t)$, but rescaled to start at unity, $\{\tau_\alpha^l, \beta^l, f_c^l\} = \{\tau_\alpha, \beta, 1\}$.

The fitting parameters used for fitting stretched exponentials to $F_{sA}(q,t)$ [Fig. 4(a)] and $F_{sA}^l(q,t)$ [Fig. 4(b)] are shown in Fig. 5; (a) relaxation times, τ_α and τ_α^l , (b) stretching parameters, β and β^l , and (c) nonergodicity parameters, f_c and f_c^l . We also show in Fig. 5(a) the fit of the asymptotic mode coupling prediction $\tau_\alpha \propto (T - T_c)^{-\gamma}$, from which we find $T_c = 0.592 \pm 0.006$ and $\gamma = 1.41 \pm 0.07$. The fitting was done without the lowest temperature, where hopping is clearly present in the system (see Fig. 2), since this type of particle motion is not included in the ideal mode coupling theory. Excluding the *two* lowest T gives a fit which is consistent with the one presented here; including all temperatures gives a considerably worse fit. Applying the same procedure to the inverse diffusion coefficient, $D^{-1}(T)$, gives $T_c = 0.574 \pm 0.005$ and $\gamma = 1.40 \pm 0.09$ (data not shown).

Also shown in Fig. 5 as insets are τ_α^l vs τ_α and β^l vs β . Within the error bars we find that τ_α and τ_α^l are identical at all temperatures. At the highest temperatures β is poorly defined since there is no well-defined plateau in $F_{sA}(q,t)$. Consequently it is difficult to compare β and β^l at high T , but we find that they become identical (within the error bars) at low T . Thus at low temperatures our results confirm the expectation that the inherent dynamics is simply a coarsening of the true dynamics, i.e., that $\{\tau_\alpha^l, \beta^l\} = \{\tau_\alpha, \beta\}$. On the other hand, the nonergodicity parameters f_c and f_c^l [Fig. 5(c)] are strikingly different. While f_c is roughly independent of T , f_c^l increases towards unity as T approaches our lowest temperature. The fact that we observe a temperature dependence of f_c^l approaching unity as T approaches our lowest temperature $T = 0.59$, leads us to conclude that this is close to the crossover temperature, T_x . We note that Goldstein's estimate of shear relaxation times at T_x (10^{-9} s) in our LJ units corresponds to 3×10^3 , which is the same order of magnitude as τ_α in the temperature range where f_c approaches unity.

Below T_x the inherent dynamics can be thought of as the true dynamics with the effect of the vibrations removed, as shown above. How should the inherent dynamics be interpreted *above* T_x ? In Fig. 4(b) the short time relaxation of the inherent self intermediate scattering function at high temperatures is seen to be approximately logarithmic in time. This is an artificial relaxation introduced by applying the

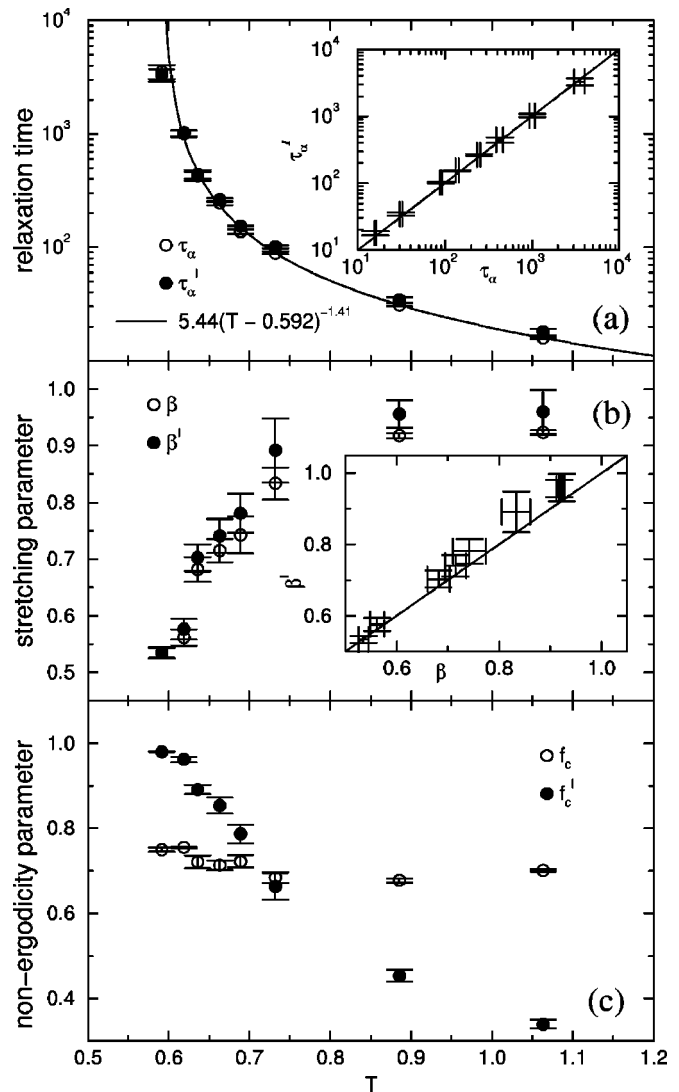


FIG. 5. Parameters describing the fit of $F_{sA}(q=7.5,t)$ and $F_{sA}^l(q=7.5,t)$ to stretched exponentials from Figs. 3(a) and 3(b), respectively. (a) Relaxation times τ_α and τ_α^l vs T . The solid line is a fit to $\tau_\alpha \propto (T - T_c)^{-\gamma}$ excluding the lowest T in the fitting (see text). (Inset) τ_α^l vs τ_α . (b) Stretching parameters β and β^l vs T . (Inset) β^l vs β . (c) Nonergodicity parameters f_c and f_c^l vs T . Error bars are estimated from deviations between three independent samples. Similar behavior is found for the B particles.

quenching procedure at a temperature where the dynamics is *not* separated into vibrations around, and transitions between inherent structures, i.e., the quenching procedure is doing more than simply removing the vibrations around inherent structures. Presumably the inherent dynamics above T_x contains information about the underlying potential energy landscape. At the present, however, we do not know how to interpret this, and we do not have an explanation as to why the (artificial) initial relaxation appears to be logarithmic at high temperatures.

We now proceed to discuss Angell's proposal, that $T_x \approx T_c$. We find that both estimated values for T_c [0.592 ± 0.005 from $\tau_\alpha(T)$ and 0.574 ± 0.005 from $D^{-1}(T)$] are in the temperature range where f_c^l is approaching unity. We note that in the system investigated here two of the asymptotic predictions of the ideal mode coupling theory do not hold; τ_α and D^{-1} have different temperature dependence

and we do not find time-temperature superposition of the α -part of the self intermediate scattering function. However, the argument given by Angell⁷ (and Sokolov²⁰) only relates to T_c as the temperature where power-law fits to experimental data tend to break down, i.e., the “usage” of MCT in this argument is similar to the way we have estimated T_c in Fig. 5(a), and does not require, e.g., time-temperature superposition.

Using the concept of inherent dynamics we have thus found evidence that for $T \leq T_x \approx T_c$ the dynamics is dominated by transitions over energy barriers. Using molecular dynamics simulations of a binary Lennard-Jones mixture it was demonstrated by Sastry *et al.* (Ref. 13) that the regions of the potential energy landscape a liquid explores depends on temperature. In particular, Sastry *et al.* studied the average inherent structure energy, $\langle E^I(T) \rangle$, found when quenching an equilibrated liquid at the temperature T . $\langle E^I(T) \rangle$ was found to be (roughly) constant above a temperature T_A , whereas it decreases when the liquid is cooled below T_A , i.e., the liquid explores deeper and deeper lying regions of the potential energy landscape. The temperature T_A was found to be well above the estimated value of the mode-coupling critical temperature T_c , and it was found to coincide with the onset of non-exponential relaxation. We find similar behavior in the system investigated here, with $T_A \approx 1.0$. The temperature dependence of $\langle E^I(T) \rangle$ is related to the configurational entropy $S_{\text{conf}}(E^I) \equiv k_B \ln[\Omega(E^I)\delta E^I]$, where $\Omega(E^I)\delta E^I$ is the number of inherent structures between E^I and $E^I + \delta E^I$. $S_{\text{conf}}(E^I)$ has recently been calculated by 3 independent groups.^{16–18} It was found that below a crossover temperature larger than T_c and close to T_A , the total entropy of the system is well approximated by the sum of independent contributions from the configurational and the vibrational entropy, respectively. Thus, from this “thermodynamic” approach, one finds a crossover temperature that is considerably higher than the crossover temperature found when using the inherent dynamics approach presented here. These two approaches are complementary, and probe different aspects of the potential energy landscape. Our results may be more closely related to results found using instantaneous normal mode analysis.^{11,32} For a soft sphere system it was found³² that the number of extended unstable normal modes becomes very small close to T_c . Similar results were found for water (the SPC/E model).¹¹ These results were interpreted as indicating that at T_c the dynamics become dominated by potential energy barriers, which is consistent with the results presented here.

IV. TRANSITIONS BETWEEN INHERENT STRUCTURES

As shown in the previous section, separation of the dynamics into vibrations around and transitions between (the basin of attraction of) inherent structures becomes possible as T approaches T_x , which is close to our lowest simulated temperature $T=0.59$. At this temperature, it therefore becomes meaningful to examine the details of the transitions between successive inherent structures. We identify such transitions by quenching the MD configurations every 0.1τ (i.e., every 10 MD-steps) and looking for signatures of the

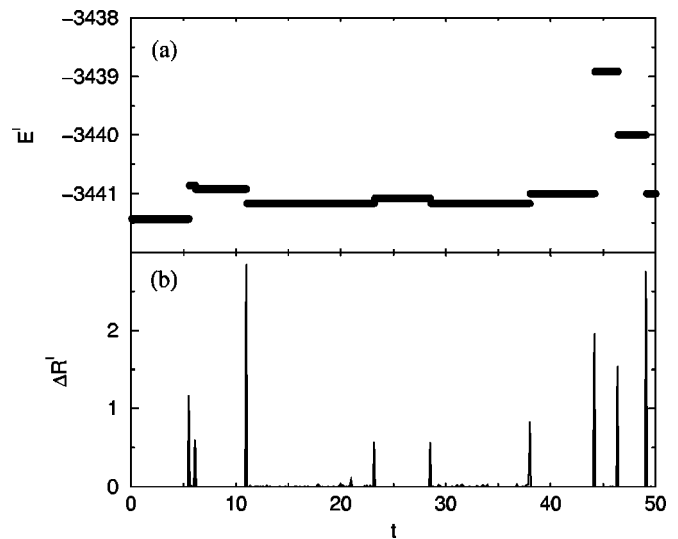


FIG. 6. Identifying transitions between inherent structures. (a) The inherent structure energy $E^I(t)$ vs time. (b) ΔR^I [Eq. (4.1)] vs time. A transition between (the basin of attraction of) two inherent structures is indicated by a jump in $E^I(t)$ and a corresponding peak in $\Delta R^I(t)$.

system undergoing a transition from one inherent structure to another. We have considered two such signatures; (i) We monitor the inherent structure energy $E^I(t)$ as a function of time, as shown in Fig. 6(a). (ii) We monitor the distance in configuration space $\Delta R^I(t)$ between two successive quenched configurations³³ [Fig. 6(b)], where

$$\Delta R^I(t) \equiv |\mathbf{R}^I(t+0.1) - \mathbf{R}^I(t)| \quad (4.1)$$

$$= \sqrt{\sum_{j=1}^N (\mathbf{r}_j^I(t+0.1) - \mathbf{r}_j^I(t))^2}. \quad (4.2)$$

Each jump in $E^I(t)$ corresponds to a peak in $\Delta R^I(t)$, indicating a transition to a new inherent structure. In the (rare) event where a transition occurs between two inherent structures with the same energy, $\Delta R^I(t)$ will still exhibit a peak even in the absence of a jump in $E^I(t)$, and for this reason we use $\Delta R^I(t)$ to identify transitions. The condition $\Delta R^I(t) > 0.1$ was found to be a sufficient threshold for this purpose. When evidence of a transition was found in a time interval $\Delta t = 0.1\tau$, this time interval was divided into 10 sub-intervals of $\Delta t = 0.01\tau$ and the procedure described above was repeated.

For each transition, we monitor the difference between the particle positions in the two successive inherent structures. The distribution $p(r)$ of all such particle “displacements” averaged over the 12 000 transitions we have identified is shown in Fig. 7. While many particles move only a small distance ($r < 0.2$) during a transition from one inherent structure to the next, a number of particles move farther, and in particular, we find that the distribution for $r > 0.2$ is to a good approximation exponential. At present we have no explanation of the origin of the exponential decay in the tail of $p(r)$ (if this is indeed the true functional form). The dotted curve is a fit to a power law with exponent $-5/2$, which is a prediction from linear elasticity theory,³⁴ describing the displacements of particles in the surroundings of a local rearrangement “event.” This power-law fit does not look very

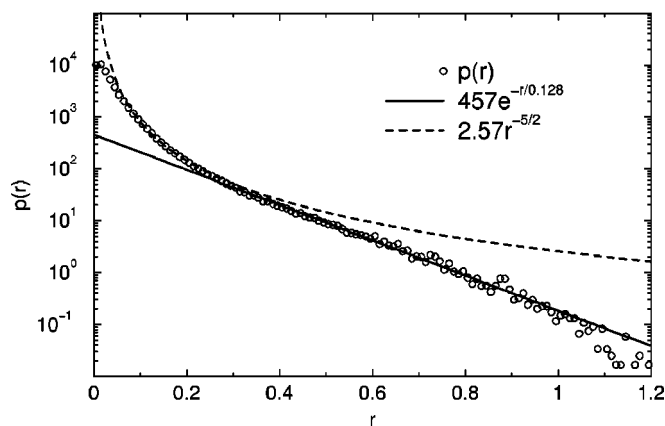


FIG. 7. Distribution of particle displacements during transitions between successive inherent structures at $T=0.59$. The integral of the distribution is normalized to be the number of particles $N=500$. Full curve is a fit to an exponential, for $0.3 < r < 1.0$. The dotted curve is a fit to a power law with (fixed) exponent $-5/2$ (Ref. 34) for $0.1 < r < 0.2$.

convincing by itself, but we note that the exponent was not treated as a fitting parameter (i.e., only the prefactor was fitted), and the power law *must* break down for small displacements, since these correspond to distances far away from the local event, and are thus not present in our relatively small sample. From the change in behavior of $p(r)$ at $r \approx 0.2$, it is reasonable to think of particles with displacements larger than 0.2 as those taking part in the local event, and the rest of the particles as merely “adjusting” to the local event. (Note however, that our data do not imply what is cause and what is effect, or even if such a distinction is meaningful.) Using this definition we find that on average approximately 10 particles participate in an event.

Figure 7 has two important consequences with regards to points discussed earlier in this paper. The first point relates to the single particle hopping indicated by the secondary peak in $4\pi r^2 G_s(r,t)$ (Fig. 2) at low temperatures. A common interpretation of the single particle hopping is that the jump of a particle from one “localized state” (first peak) to the second localized state (secondary peak), corresponds to the transition of the system over an energy barrier from one inherent structure to the next. If such a transition typically occurs over a single energy barrier, i.e., without any new inherent structures between the two states, we would expect to find a preference for displacements of one average interparticle distance ($r \approx 1$) in Fig. 7. That this is *not* the case demonstrates that the hopping indicated by the secondary peak in $4\pi r^2 G_s(r,t)$ at low temperatures is *not* due to transitions over single energy barriers. Instead, as seen in the inherent trajectory in Fig. 3, the jump occurs via a number of “intermediate” inherent structures.

The second important consequence of Fig. 7 is that particles in the surroundings of a local event are displaced by small distances. This kind of motion is difficult to detect in the true dynamics, since it is dominated by the thermal vibrations. Presumably this kind of motion is the reason why the inherent trajectory in Fig. 3 shows small displacements ($\lesssim 0.2\sigma_{AA}$), even when the corresponding true trajectory seems to vibrate around the same position. When a transition

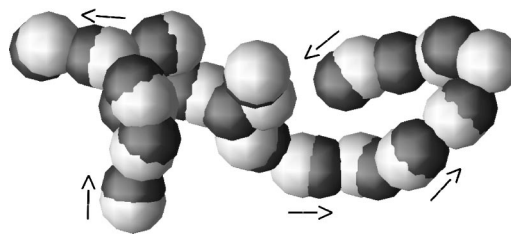


FIG. 8. Before (light) and after (dark) one typical transition, all the particles which move a distance greater than $0.2\sigma_{AA}$. Particles are shown with a diameter of σ_{AA} . Note that most particles move considerably *less* than σ_{AA} (compare Fig. 7). The cooperative, stringlike nature of the particle motions during the interbasin transition can be clearly seen.

between inherent structures involving significant particle rearrangements in the surroundings occurs, the particle starts vibrating around a position that is slightly displaced, and a corresponding small displacement of the inherent trajectory is seen. This view of the dynamics is also consistent with the fact that the first peak in the inherent counterpart of $4\pi r^2 G_s(r,t)$ (not shown, see Ref. 24) is not a delta function in $r=0$.

By observing, for a number of transitions, the positions of all particles that moved a distance greater than 0.2 during a transition, we find these particles to be clustered together in “strings,” as shown in Fig. 8. Typically, one transition appears to involve just one stringlike cluster. Detailed investigations of the transition events will be presented in a separate publication. Here we simply note that stringlike particle motion has been observed also in the true dynamics above T_c in a similar binary Lennard-Jones mixture.³⁵ Those strings are found on long time scales and involve particles moving approximately one interparticle distance, and are thus different from, but presumably related to, the strings found in the present work.

V. CONCLUSIONS

We have investigated the dynamics of a model glass-forming liquid in terms of its potential energy landscape by “quenching” a time series of MD configurations to a corresponding time series of inherent structures. In this way we have provided numerical evidence for the conjecture, originally made by Goldstein 30 years ago in this journal,⁵ that below a crossover temperature T_x the dynamics of the liquid can be separated into vibrations around and transitions between inherent structures. Specifically, by comparing the self-intermediate scattering function $F_s(q,t)$ with its inherent counterpart $F_s^I(q,t)$ we presented evidence for the existence of T_x . It is perhaps not surprising that the dynamics of a liquid becomes dominated by the structure of the potential energy landscape at sufficiently low temperatures. What we have done here using the concept of inherent dynamics, is to provide direct numerical evidence for this, *and* we have shown that this regime can be reached by equilibrium molecular dynamics (for the particular system investigated here). To our knowledge this is the first time such evidence has been presented.

In agreement with previous proposals^{7,20,21} we find $T_x \approx T_c$, where T_c is estimated from a power-law fit to τ_α .

This is also the temperature range where single particle hopping starts to dominate the dynamics, and τ_α becomes on the order of 10^{-9} s (Goldstein's estimate of the shear relaxation time at T_x).

The fact that we have been able to cool the system, under equilibrium conditions, to temperatures where the separation between vibrations around inherent structures and transitions between these is (almost) complete, means that it becomes meaningful to study the individual transitions over energy barriers, since the transitions in this regime dominate the dynamics. Our two key findings with regards to the individual transitions between inherent structures are (i) single particle displacements during transitions show no preference for displacements on the order of the interparticle distance, showing that the single particle hopping indicated in $4\pi r^2 G_s(r,t)$ at low T (Fig. 2) does *not* correspond to transitions of the system over single energy barriers; and (ii) particle displacements during transitions are spatially correlated in "strings."

ACKNOWLEDGMENTS

We thank F. Sciortino and F. H. Stillinger for helpful feedback. This work was supported in part by the Danish Natural Science Research Council.

¹F. H. Stillinger, *Science* **267**, 1935 (1995).

²C. A. Angell, *Science* **267**, 1924 (1995).

³H. Frauenfelder, S. G. Sligar, and P. G. Wolynes, *Science* **254**, 1598 (1991).

⁴P. G. Wolynes, J. N. Onuchic, and D. Thirumalai, *Science* **267**, 1619 (1995).

⁵M. Goldstein, *J. Chem. Phys.* **51**, 3728 (1969).

⁶F. H. Stillinger and T. A. Weber, *Phys. Rev. A* **28**, 2408 (1983).

⁷C. A. Angell, *J. Phys. Chem. Solids* **49**, 863 (1988).

⁸F. H. Stillinger, *J. Chem. Phys.* **88**, 7818 (1988).

⁹R. J. Speedy, *J. Chem. Phys.* **100**, 6684 (1994); R. J. Speedy and P. G.

DeBenedetti, *Mol. Phys.* **88**, 1293 (1996); R. J. Speedy, *ibid.* **95**, 169 (1998).

¹⁰C. Dasgupta and O. T. Valls, *Phys. Rev. E* **53**, 2603 (1996); **59**, 3123 (1999).

¹¹F. Sciortino and P. Tartaglia, *Phys. Rev. Lett.* **78**, 2385 (1997); E. La Nave, A. Scala, F. W. Starr, F. Sciortino, and H. E. Stanley, *ibid.* **84** (in press).

¹²A. Heuer, *Phys. Rev. Lett.* **78**, 4051 (1997); S. Büchner and A. Heuer, *ibid.* **84**, 2168 (2000).

¹³S. Sastry, P. G. DeBenedetti, and F. H. Stillinger, *Nature* **393**, 554 (1998).

¹⁴M. Schulz, *Phys. Rev. B* **57**, 11319 (1998).

¹⁵L. Angelani, G. Parisi, G. Ruocco, and G. Vilianni, *Phys. Rev. Lett.* **81**, 4648 (1998); *Phys. Rev. E* **61**, 1681 (2000).

¹⁶F. Sciortino, W. Kob, and P. Tartaglia, *Phys. Rev. Lett.* **83**, 3214 (1999).

¹⁷B. Coluzzi, M. Mezard, G. Parisi, and P. Verrocchio, *J. Chem. Phys.* **111**, 9039 (1999); B. Coluzzi, G. Parisi, and P. Verrocchio, *Phys. Rev. Lett.* **84**, 306 (2000); *J. Chem. Phys.* **112**, 2933 (2000).

¹⁸S. Büchner and A. Heuer, *Phys. Rev. E* **60**, 6507 (1999).

¹⁹W. Götze and L. Sjogren, *Rep. Prog. Phys.* **55**, 241 (1992).

²⁰A. P. Sokolov, *J. Non-Cryst. Solids* **235–237**, 190 (1998).

²¹T. R. Kirkpatrick and D. Thirumalai, *Phys. Rev. B* **36**, 5388 (1987); T. R. Kirkpatrick and P. G. Wolynes, *ibid.* **36**, 8552 (1987); T. R. Kirkpatrick, D. Thirumalai, and P. G. Wolynes, *Phys. Rev. A* **40**, 1045 (1989).

²²A. Cavagna, I. Giardina, and G. Parisi, *Phys. Rev. B* **57**, 11251 (1998).

²³S. Franz and G. Parisi, *Phys. Rev. Lett.* **79**, 2486 (1997); M. Cardenas, S. Franz, and G. Parisi, *J. Chem. Phys.* **110**, 1726 (1999).

²⁴T. B. Schröder and J. C. Dyre, *J. Non-Cryst. Solids* **235–237**, 331 (1998).

²⁵W. H. Press *et al.*, *Numerical Recipes* (Cambridge University Press, Cambridge, 1986).

²⁶J.-P. Hansen and I.R. McDonald, *Theory of Simple Liquids* (Academic, London, 1986).

²⁷J.-N. Roux, J.-L. Barrat, and J.-P. Hansen, *J. Phys.: Condens. Matter* **1**, 7171 (1989).

²⁸G. Wahnström, *Phys. Rev. A* **44**, 3752 (1991).

²⁹F. Yonezawa and S. Fujiwara, *Mater. Sci. Eng., A* **178**, 23 (1994).

³⁰S. R. Kudchadkar and J. M. Wiest, *J. Chem. Phys.* **103**, 8566 (1995).

³¹F. Sciortino, P. Gallo, P. Tartaglia, and S.-H. Chen, *Phys. Rev. E* **54**, 6331 (1996).

³²S. D. Bembenek and B. B. Laird, *J. Chem. Phys.* **104**, 5199 (1996).

³³I. Ohmine, *J. Phys. Chem.* **99**, 6767 (1995).

³⁴J. C. Dyre, *Phys. Rev. E* **59**, 2458 (1999).

³⁵C. Donati, J. F. Douglas, W. Kob, S. J. Plimpton, P. H. Poole, and S. C. Glotzer, *Phys. Rev. Lett.* **80**, 2338 (1998).